HAL
open science

Line list of 12CH4 in the 4300–4600 cm–1 region

Andrei V Nikitin, A.A. A Rodina, X. Thomas, L. Manceron, L. Daumont, M. Rey, K. Sung, A.E. E Protasevich, S.A. A Tashkun, I.S. S Chizhmakova, et al.

▶ To cite this version:

Andrei V Nikitin, A.A. A Rodina, X. Thomas, L. Manceron, L. Daumont, et al.. Line list of 12CH4 in the 4300–4600 cm–1 region. Journal of Quantitative Spectroscopy and Radiative Transfer, 2020, 253, pp.107061. 10.1016/j.jqsrt.2020.107061 . hal-03045996

HAL Id: hal-03045996

https://hal.science/hal-03045996v1

Submitted on 8 Dec 2020

HAL is a multi-disciplinary open access archive for the deposit and dissemination of scientific research documents, whether they are published or not. The documents may come from teaching and research institutions in France or abroad, or from public or private research centers.

L'archive ouverte pluridisciplinaire **HAL**, est destinée au dépôt et à la diffusion de documents scientifiques de niveau recherche, publiés ou non, émanant des établissements d'enseignement et de recherche français ou étrangers, des laboratoires publics ou privés.

Line list of $^{12}CH_4$ in the 4300-4600 cm^{-1} region

A.V. Nikitin[1], A.A. Rodina[1], X. Thomas[2], L. Manceron[3,4], L. Daumont[2], M. Rey[2], K. Sung[5], A.E. Protasevich[1], S.A. Tashkun[1], I. S. Chizhmakova[6] Vl. G. Tyuterev[2,7]

[1.] *V.E. Zuev Institute of Atmospheric Optics, Russian Academy of Sciences, 1, Akademichesky Avenue, 634055 Tomsk, Russian Federation*
[2.] *Groupe de Spectrométrie Moléculaire et Atmosphérique, UMR CNRS 6089, Université de Reims, U.F.R. Sciences, B.P. 1039, 51687 Reims Cedex 2, France*
[3.] *AILES Beamline, Synchrotron SOLEIL, L'Orme des Merisiers, St-Aubin BP48, F-91192 Gif-sur-Yvette Cedex*,France.
[4.] Sorbonne Université, CNRS, MONARIS, UMR 8233, 4 place Jussieu, Paris, France
[5.] *Jet Propulsion Laboratory, California Institute of Technology, 4800 Oak Grove Drive, Pasadena, CA 91109, USA*
[6] *Institute of Monitoring of Climatic and Ecological Systems, Russian Academy of Sciences , 10/3, Academichesky avenue, 634055, Tomsk, Russian Federation*

[7] *QUAMER,Tomsk State University, 36 Lenin Avenue, 634050 Tomsk, Russian Federation*

Number of Pages: 22
Number of Figures: 8
Number of Tables: 5
Number supplemental files: 1

Running Head: $^{12}CH_4$ absorption in the 4300-4600 cm^{-1} range

Keywords: high resolution spectra; CH_4; methane; Octad; long path FTIR, vibration-rotation states; intensities; infrared absorption; effective Hamiltonian.

Correspondence should be addressed to:
Andrei V. Nikitin,
*Laboratory of Theoretical Spectroscopy, V.E. Zuev Institute of Atmospheric Optics, SB RAS, 1, Academician Zuev square, 634055, Tomsk, Russia
E-mail: avn@iao.ru
Tel. +73822 – 491111, ext. 1260

Abstract

Four spectra of normal samples of CH_4 in the 4300-4600 cm^{-1} region were recorded by using a Fourier transform spectrometer in Reims, France at long paths (202 m, 602 m, 1604 m, and 1804 m) and different pressures. Additional spectra of $^{12}CH_4$ covering the same region were obtained at 80-123 K, and 93 m path length at SOLEIL Synchrotron in Paris for different pressures and were used to measure low-J lines. Line positions and intensities were retrieved by non-linear least-squares curve-fitting procedures and analyzed using effective Hamiltonian and effective dipole transition moment models. A new measured line list contains positions and intensities for 14151 absorption features. Quantum assignments were made for more than 10304 transitions of $^{12}CH_4$, which represent ~99% of the integrated line intensity observed in this region. Some 1699 hot band transitions for (Dyad – Tetradecad) system were assigned. The resulting list of lines is significantly more accurate than previous empirical compilations. Positions of 8605 cold band transitions for (GS – Octad) system were fitted with an RMS standard deviation of 0.0014 cm^{-1}. The sum of observed intensities between 4300 and 4600 cm^{-1} fell within 8% of the predicted value from ab initio variational calculations reported in the TheoReTS database (http://theorets.univ-reims.fr ; http://theorets.tsu.ru).

Highlights

1. 14151 line positions and intensities were retrieved in the 4300- 4600 cm^{-1} region.
2. More than 7000 new assignments were made in the region.
3. 8605 experimental line positions were modeled to 0.0014 cm^{-1}.
4. 5402 experimental line intensities at 296 K were modeled to 9.9% *rms.*

1. Introduction

The aim of the present work is to improve the line list and to extend the assignments of weak and hot band transitions of $^{12}CH_4$ in the 4300 - 4600 cm^{-1} region of the Octad [1] [2] [3] [4] [5]. The Octad band system (24 upper state vibrational sublevels) has been first studied by Hilico et al. [1] who also considered some hot bands [6] [7] for lower polyads of methane. The Octad assignments have been extended in Refs. [2] , [4] and a list of strong lines in the 4300-4600 cm^{-1} range for atmospheric applications has been published in Ref [8]. The present analysis is a continuation of a series of works [4], [5] using Fourier Transform spectra with long optical paths and represents a considerable improvement over previous works [1], [2].

Over decades, a better knowledge of methane infrared spectra has been demanded for various atmospheric and astrophysical applications [9], [10], [11]. This task was motivated by new challenges related to remote sensing of planetary atmospheres. Among them, many studies have been focused on the study of radiative properties of the Titan atmosphere (Saturn's largest satellite), which is composed of 98.6% nitrogen and 1.4% methane at temperatures ranging between 70 K and 200 K [12] [13] [14] [15] [16] [17]. Reliable parameters of methane absorption and emission bands are essential for accurate interpretation of the IR spectra provided by orbiting and ground-based observatories [18], [19], [20], [21], [22]. The insufficient coverage and accuracy of spectral data became a major issue for investigations of outer planets [23] [14] [15]. Despite recent progress [3] [24] [25] [8] [26] [27] [4] [28] [5] in the methane modeling, available line lists [29] [30] [31] [32] [33] [34] [35] based on laboratory measurements do not yet provide all necessary information to reproduce atmospheric methane spectra in the near infrared. This is particularly the case of relatively weak absorption bands that significantly contribute to the absorption at long optical paths of planetary atmospheres [36].

Because of high tetrahedral symmetry, some normal modes of methane are doubly or triply degenerate in the harmonic approximation and fall within nearby intervals. Additionally, there are accidental resonances due to near coincidence of fundamental vibrational frequencies and of their combinations ($\omega_1 \cong \omega_3 \cong 2\omega_2 \cong 2\omega_4$) that results in grouping vibrational levels into so-called polyads (Dyad, Pentad, Octad, etc…) [37]. The vibrational energy levels with the same polyad number $P = 2\,V_1 + V_2 + 2\,V_3 + V_4$ calculated from the four vibrational quantum numbers fall within the same energy range. In this work, we study the methane spectra belonging to the Octad band system with P=3. The scheme of $^{12}CH_4$ vibrational states is shown in Figure 1. The blown-up scale at the right-hand side represents the sub-band centers with their symmetry types, which are studied in the present work.

At room temperature, our observed line positions and intensities agree with a series of experimental lines reported in[2] [4] within experimental accuracy and could be well reproduced by our theoretical model. However, in some intervals of the $^{12}CH_4$ Octad , the calculated line lists included in the databases [29] [30] cannot be used for modeling spectra at temperatures that considerably differ from 296 K. In the nearby ranges 4600-4850 cm^{-1} and 3760-4100 cm^{-1} ranges, the accuracy of spectra modeling was considerably better than that in the 4100-4600 cm^{-1} range, which is the subject of the present work. Erratic behaviors of some line intensities at temperatures other than room temperature could be due to incorrect quantum assignments of experimental transitions in the past and to wrong lower level energy values. On the whole, in the Tetradecad range, the linelist was recently composed and updated simultaneously with the improved assignments [38] [39] [40]. This was not the case of the Octad range, where the list of transitions had been compiled before high-accuracy effective models became available [2] [4] [41]. A lot of observed line positions and intensities have been reported in Ref. [2], but the authors did not aim at providing a complete list of the observed and assigned transitions. Furthermore, the spectra of methane isotopologues and hot transitions of (Tetradecad – Dyad) band system, which fall in the same range, had not been available at the time of previous publications. Without this information, the full assignment of weak $^{12}CH_4$ cold band transitions was complicated. In the present work, we report an extensive list of assigned transitions in the 4300 - 4600 cm^{-1} range using experimental spectra recorded at various temperatures and path lengths. This linelist provides a more accurate description of experimental spectra at room and cold temperatures in comparison with currently available databases.

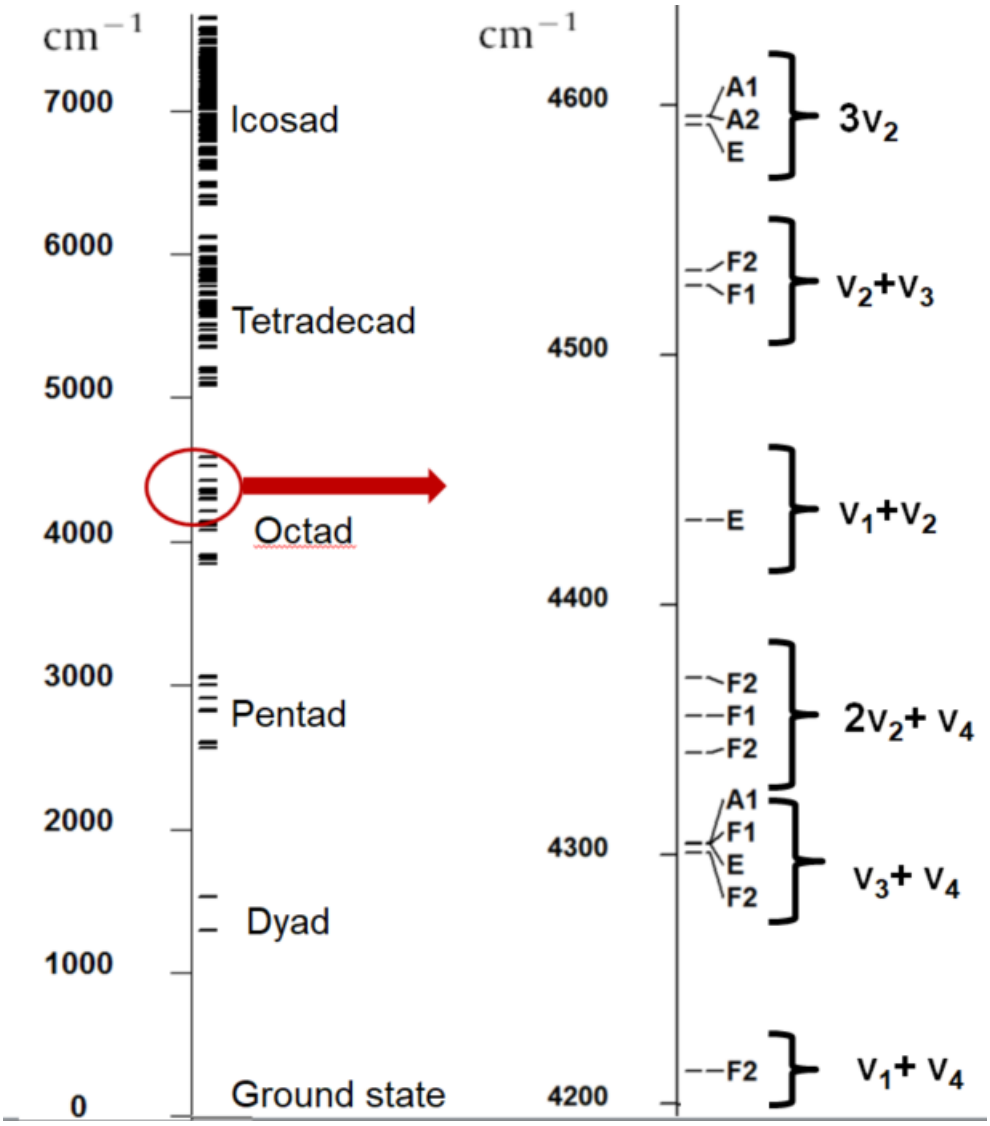

Fig. 1. *Vibrational levels of the* $^{12}CH_4$ *polyads (left side) and the vibrational sublevels of a part of Octad (right side) corresponding to rovibrational bands analyzed in this work. The right hand side panel displays the principal vibration quantum numbers* ($\upsilon_1\upsilon_2\upsilon_3\upsilon$)*, symmetry types of vibration sublevels, and vibrational ranking numbers within the Octad. The symmetry types correspond to irreducible representations of the* T_d *point group* [42] [37].

The paper is structured as follows. Experimental spectra recorded in GSMA (Reims) and SOLEIL (Paris) at 100, 113, 123 and 290 K are described in Sections 2a and 2b. Section 3 is devoted to the determination of line parameters and Section 4 to spectra assignments. Section 5 gives the information on newly assigned line lists provided in the Supplementary Materials.

2. Experiment

In this study, we used a large set of Fourier transform spectra (FTS) recorded in the GSMA Laboratory at Reims University. Some of the spectra have already been presented in former publications concerning specific studies [4, 43-45]. In the series of experimental studies, a 50 m

base multipass cell of GSMA has been optically configured to high-resolution step-by-step spectrometer as first described in [4] [5] [43] [40] [44]. The absorption path lengths were set to 202, 602, 1603 meters by adjusting the number of the transverse beams inside the 50 meters based White-type gas cell. The methane gas used to fill the cell is a natural abundance sample, and the pressures varied from 1 to 25 Torr, as described in Table 1. The spectrometer is based on the Connes principle and its apparatus function is mainly determined by the maximal optical path difference (MOPD) and by the apperture chosen at the entrance of the spectrometer. During the experiment, the average cell temperature was controlled with fluctuations in time that did not exceed two degrees.

The first series of spectra with 1600 m absorption path-length in the 1.6 μm window of methane (e.g., H-band) has been explored [45] for the Titan atmospheric spectra analysis [15]. In this work, most of the measured lines were obtained from E, F, H, I spectra (see Table 1). G and J spectra were only used to check the intensities of the weak lines. F and I spectra recorded at a pressure of 5 Torr were used to determine the positions and check the intensities of the weak lines in the 4300-4500 cm^{-1} range and to determine the positions and check the intensities of some strong lines in the 4500-4600 cm^{-1} range. The spectra E and H were only used to check the positions and intensities of the strongest lines in the region. Because of significant spatial temperature gradients within the cell for low-T conditions , the Reims spectra A, B, C were used to determine positions of weak lines only at the initial stage of work.

Table 1. Experimental conditions for the series of CH_4 spectra in the Octad range.

Spectrum ID	Iris Diameter, Focal length (mm)	Pressure (Torr)	Temperature (K)	Absorption path (m)
GSMA FTS spectra recorded in Reims				
A	4.5, 1040	3.43	110	8.52
B		4.17	113	32.52
C		3.28	113	80.52
E	4, 1040	1.06	292	201.84
F		5.03	291	
G		25.98	289	
H	4, 1040	1.05	289	602.32
I		5.08	290	
J		25.11	289	
K	3.5, 1040	1.065	289	1603
L		4.070	288	
SOLEIL FTS spectra recorded in Paris				
M	1.5, 418	0.0073	100	93.14
N		0.0019		
O		0.00159		
P		0.00155		
Q		0.00068		
R		0.00094	102	
S		0.03	112	
T		1.16	123	

Six spectra were recorded at low temperature at Synchrotron SOLEIL using the long path cryogenic cell described in reference [46] and the Bruker 125 HR interferometer. The optical path length in the cell was set to 93.14(1) meters for all these recordings. Such a long path length would make the strong lines in the region easily being saturated and subject to unwanted non-linearity effects unless the sample pressure was used sufficiently low. At the low sample pressure, however, the pressure readings of the cold cell become uncertain due to thermo-molecular effects, especially when the pressure sensor is placed outside the cell, as was the case for our setup. To avoid these possible issues, the methane sample was diluted in pure nitrogen gas in a 3L container at a 0.100(1)% mixing ratio and precisely measurable amounts (0.917 to 2.52 mbar) were introduced in the cell [47]. The mixing ratio was chosen so that nitrogen pressure broadening is not an issue here. The relative uncertainty on the methane pressure is estimated to be about 1.5%. The spectra were recorded using a Si/CaF_2 beamsplitter, a scanner optical velocity of 5.06 cm/s, a low pass filter with 40 kHz cut-off and a 120 cm maximum

optical path difference. This corresponds to 0.0075 cm^{-1} resolution, according to Bruker's definition, which is about the Doppler linewidth at this temperature. The spectra were obtained with no apodization and 2400 scans were averaged for each of them. Wavenumber calibration was carried out using both weak residual water lines and CO lines resulting from a special spectrum recording. For this spectrum, a separate mixture containing 0.0053 torr of CO with a trace amount of methane was used. For spectra M-Q, an agreement within 3% (1σ) for the CO intensities available in HITRAN-2016 [29] was obtained. The average temperature was measured in two ways: a value T= 100 ± 3 K was obtained using 12 different temperature sensors along the optical path giving about 3 K uncertainty (1σ) [46]. Secondly, using the CO 2-0 line intensities of the calibration spectrum, an average temperature of 99 ± 3K was obtained, consistent with the sensor's direct temperature measurement. In the 4300-4600 cm^{-1} range, S and T spectra recorded at 112 and 123 K were used to determine line positions and intensities for low J values mostly for weak lines. The same setup as for spectra M-Q was used for spectra R-T.

3. Line parameters in the 4300 -4600 cm-1 region

All positions and intensities have been obtained using the SpectraPlot software [48] from spectra recorded in Reims and Paris. All spectral features with intensities > 1.0×10^{-25} $cm^{-1}/(molecule\cdot cm^{-2})$ and many of the lines with intensities between 1.0×10^{-25} and 2.0×10^{-26} $cm^{-1}/(molecule\cdot cm^{-2})$ were retrieved. At the first stage, we used the same technique as described in [40]. Line parameters of low J values were obtained from Spectrum S and T at 112 and 123 K, respectively. Then, we used the fixed parameters determined from the low J lines to obtain the parameters of strong lines from the spectra recorded with the optical path L = 201.84 meters. At the next stage, we fitted weak lines using the spectra E, F, G, I, and J. The final fit was made using the six room-temperature spectra E – J and spectrum T recorded at 123 K. In this case, some positions of the low J lines were set to values previously obtained from cold spectra. Calibration of spectra A, B, and C was carried out in the similar way as in Ref. [40]. The previously observed methane lines and CO_2 transitions were used to calibrate the spectra E, F, G, H, I, and J. The CO transitions were used to calibrate the spectra K and L. For spectra A, B and C, the calibration was checked for selected residual water transitions from the HITRAN-2016 database. The average shift of these transitions was 5.0×10^{-6} cm^{-1}. When the spectra with different pressures were used for a simultaneous fitting, the self-pressure-induced line shift parameter was assumed to be the same for all lines equal to -0.013 cm^{-1}/atm [49].

The strongest lines of $^{12}CH_4$ (with intensities > $3.\times10^{-23}$ $cm^{-1}/(molecule\cdot cm^{-2})$) were almost saturated in several spectra (1 Torr, 201 meters) in the 4300-4600 cm^{-1} range. For these few transitions the previously observed lines of Ref. [1] or HITRAN-2016 [29] values were incorporated in our final line list. The corresponding 209 lines are flagged with H.

Some 8619 $^{12}CH_4$ transitions are now assigned in the 4300-4600 cm^{-1} region that is to compare with 2834 experimental transitions assigned in Refs [2] [3]. Detailed examples of newly measured and assigned transitions are shown in **Figs. 2-4** for the 4308-4513 cm^{-1} region. A comparison of observed and calculated spectra at 123 K using both the present work and HITRAN-2016 [29] line lists is shown in **Figs 5-6** for the 4338-4443 cm^{-1}range. In these examples, we compare new data with HITRAN-2016, which is the most frequently used database for atmospheric applications, but the general conclusions are also valid for other existing empirically fitted line lists. HITRAN-2016 spectroscopic database [29] contains 29009 transitions of $^{12}CH_4$ in this range with the intensity cutoff 1×10^{-29} $cm^{-1}/(molecule\cdot cm^{-2})$, only about 10% of these lines being measured and assigned in laboratory spectra [2] [3].

These comparisons show that HITRAN-2016 [29] provides correct integrated methane absorption on the entire scale, but the line-by-line list fails to reproduce spectra at low temperatures in the considered range under high resolution. It would not provide reliable simulations of methane absorption for some spectral features when the temperature conditions significantly differ from 296 K. Furthermore, **Figure 7** illustrates that, in some cases, previously available line lists inaccurately describe observed spectra in some intervals even at 296 K. As many other empirical compilations, it comprised a mixture of quite accurate laboratory measurements and extrapolations using the effective Hamiltonian and effective dipole moment models. Figures 5 and 7 illustrate that HITRAN-2016 database (and other empirical compilations as well) contains some transitions in this range, for which line positions and intensities have significant errors beyond their reported uncertainties. This mostly concerns several series of weak and medium lines with intensities in the range 3×10^{-23} - 1×10^{-24} $cm^{-1}/(molecule\cdot cm^{-2})$. An invalid assignment of transitions could lead to errors in the temperature dependence and to inaccurate interpretation of the observed transmittance in terrestrial and planetary atmospheric for some spectral intervals.

A sample of seventeen isolated lines observed in this work (TW) with intensities in the range [1×10^{-24} - 3×10^{-23}] $cm^{-1}/(molecule\cdot cm^{-2})$ is listed in **Table 2**. The third column shows the intensities ratio from HITRAN-2016 line list, ratioed to the corresponding intensities of this work in the third column. The fourth column gives the ratio of *ab initio* line intensity to that measured in this work. Initially, these theoretical predictions were obtained using *ab initio*

ACVQZ dipole moment surface [50] and global variational calculations [51] [52] [53] as included in the TheoReTS information system [54]. Some lines listed in **Table 2** were considered 'unstable' in terms of the classification described in Ref [55] due to sharp accidental resonances. In the last column of Table 2, the corresponding outliers of variational calculations were smoothed using accurate wavefunctions of the optimaised EH. Table 2 shows that the intensities obtained in this work for the seventeen relatively strong lines listed are much closer to the best available ab initio intensities [54] and 7% higher than those HITRAN-2016 [29] [1].

Table 2. Example of intensities for seventeen isolated lines in the 4300 - 4600 cm^{-1} region.

Line position[a]	Line intensity This work[b]	Intensity ratio to TW	
		HITRAN-2016	Ab initio [c]
4309.370639	15.61	0.86	0.98
4338.140149	6.999	0.54	0.99
4353.040613	17.28	1.06	0.88
4391.662283	4.798	0.93	0.91
4415.850673	15.57	0.59	0.96
4418.536734	19.12	0.86	1.00
4425.295494	18.67	0.83	0.98
4455.944122	63.21	1.20	1.06
4502.424255	62.86	1.00	1.01
4508.039449	22.22	0.96	0.98
4508.413075	41.06	0.98	1.02
4560.096669	2.887	0.74	1.05
4560.374781	21.53	1.28	0.97
4569.715772	16.46	0.99	1.00
4577.868249	46.67	1.08	1.04
4588.477338	13.37	0.98	1.02
4588.704137	11.74	0.96	0.97
Average ratio		0.93	0.99

Notes:
[a] *wavenumber measured in this work [cm^{-1}].*
[b] *intensity measured in this work in 10^{-24} cm^{-1}/(molecule·cm^{-2})*
[c] *with corrected outliers of "unstable lines " (see the text)*

The integrated intensities (obtained by summation of intensities of all lines) in the range 4300-4600 cm^{-1} are shown in **Table 3**. The integrated intensities of our observed line list are close to the integrated intensities of HITRAN-2016 [29]. The integrated intensities of [54] and GEISA [30] appear to be larger by 5-7% than those of this work. There are two factors contributing to this difference: greater intensities of the strong and intermediately strong lines and much larger number of weak lines incorperated in full variational calculations [54]. The average absolute uncertainty of the intensities measured in this work is estimated as 5-10%. The factors

influencing the accuracy include temperature fluctuations of ~ 1.5 degrees and a large aperture of 3-5 mm for the Reims spectrum sets. Considerable numbers of transitions with intensities below 1×10^{-24} cm^{-1} / (molecule · cm^{-2}) are found to be blended, and an empirical determination of transition intensity strongly depends on the neighboring lines. In many cases, the lower J was not known, and a default lower state energy value of 814.6 cm^{-1} was used. Since the Reims spectra were recorded at a temperature of T = 291 K, recalculation of the intensities of such transitions at T = 296 K could be incorrect for the unassigned lines. Note, that the 113 K spectrum was particularly useful for transitions blended by higher J lines in the room temperature spectra. However, for more accurate measurement of intensities, further extension of assignments and recording of spectra with a shorter optical path and better temperature stabilization is necessary.

Table 3. Integrated methane intensities in the range 4300-4600 cm^{-1}

Source	#lines	S Int*
This work : observed intensities	14151	3.98***
This work : calculated from empirically fitted EDM model	24221	3.90
This work: calculated from ab initio based EDM intensities (EDM fitted to variational intensities [54] computed using ACVQZ dipole moment)	23812	4.21
Full variational ab initio based list [54] **	286635	**4.20**
HITRAN-2016 [29] ($^{12}CH_4$ only)	29009	4.09
GEISA-2015 [30]	22127	4.18

* Sums of line intensities (10^{-19} cm/molecule)

** Ab initio intensities computed with ACVQZ DMS [55], see TheoReTS [54] including hot bands (for natural $^{12}CH_4$ abundance)

*** contains $^{13}CH_4$

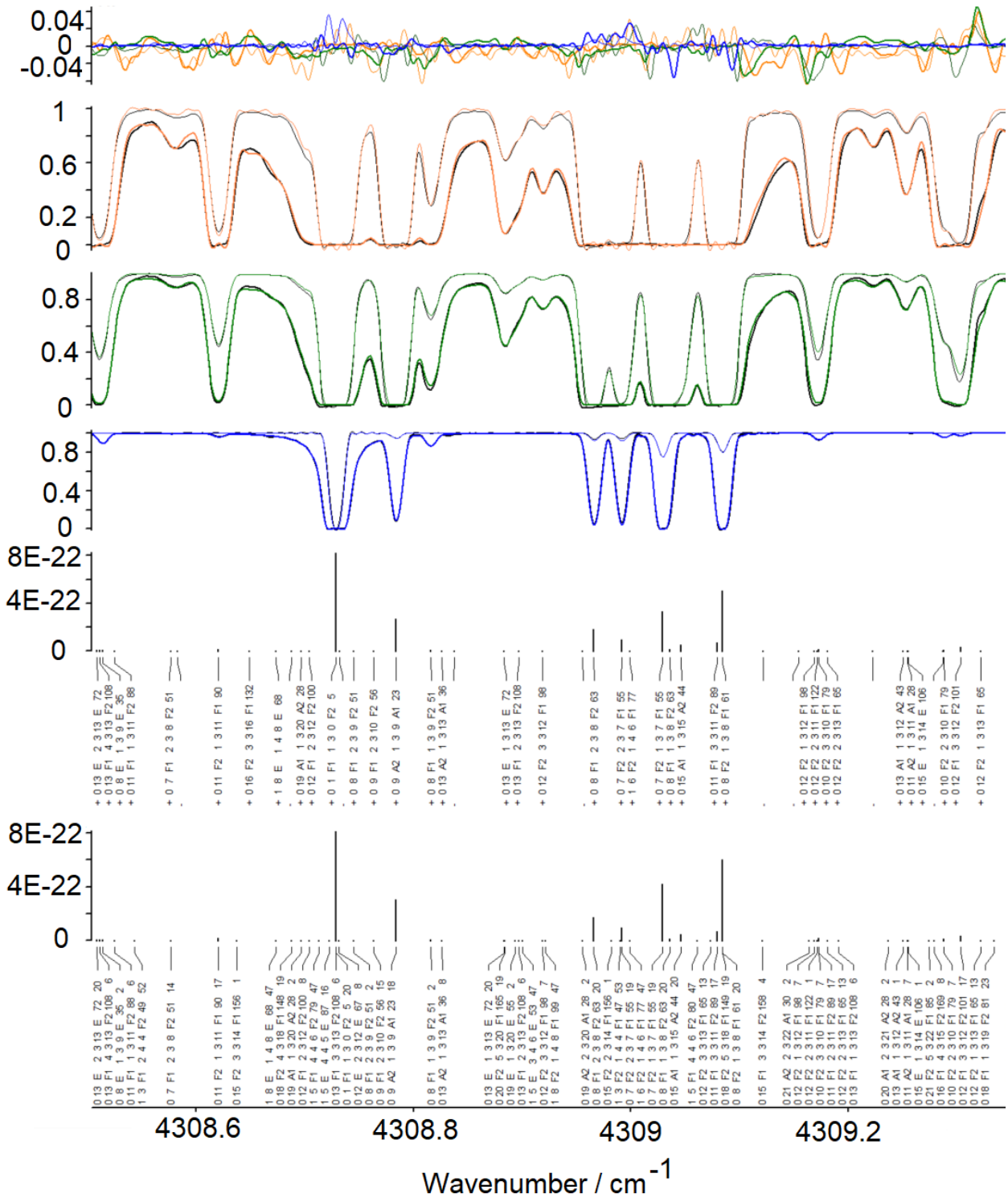

Fig. 2. *Example of quantum number assignments in the $^{12}CH_4$ spectra. The upper panel shows residuals (obs-calc) for three spectra (orange 602 m at 289 K and green Reims 201 meter spectra at 291 K, blue S, T cold spectra). Next panel below shows 602 meter (black) and two calculated spectra (orange). Next panel below shows the 201 meter observed spectrum in black, two calculated 201 m spectra (green). Next panel S, T shows observed spectra and two corresponding calculated spectra. Next panel shows assigned experimental line sticks and the lowest panel – our calculated intensity sticks at 296 K.*

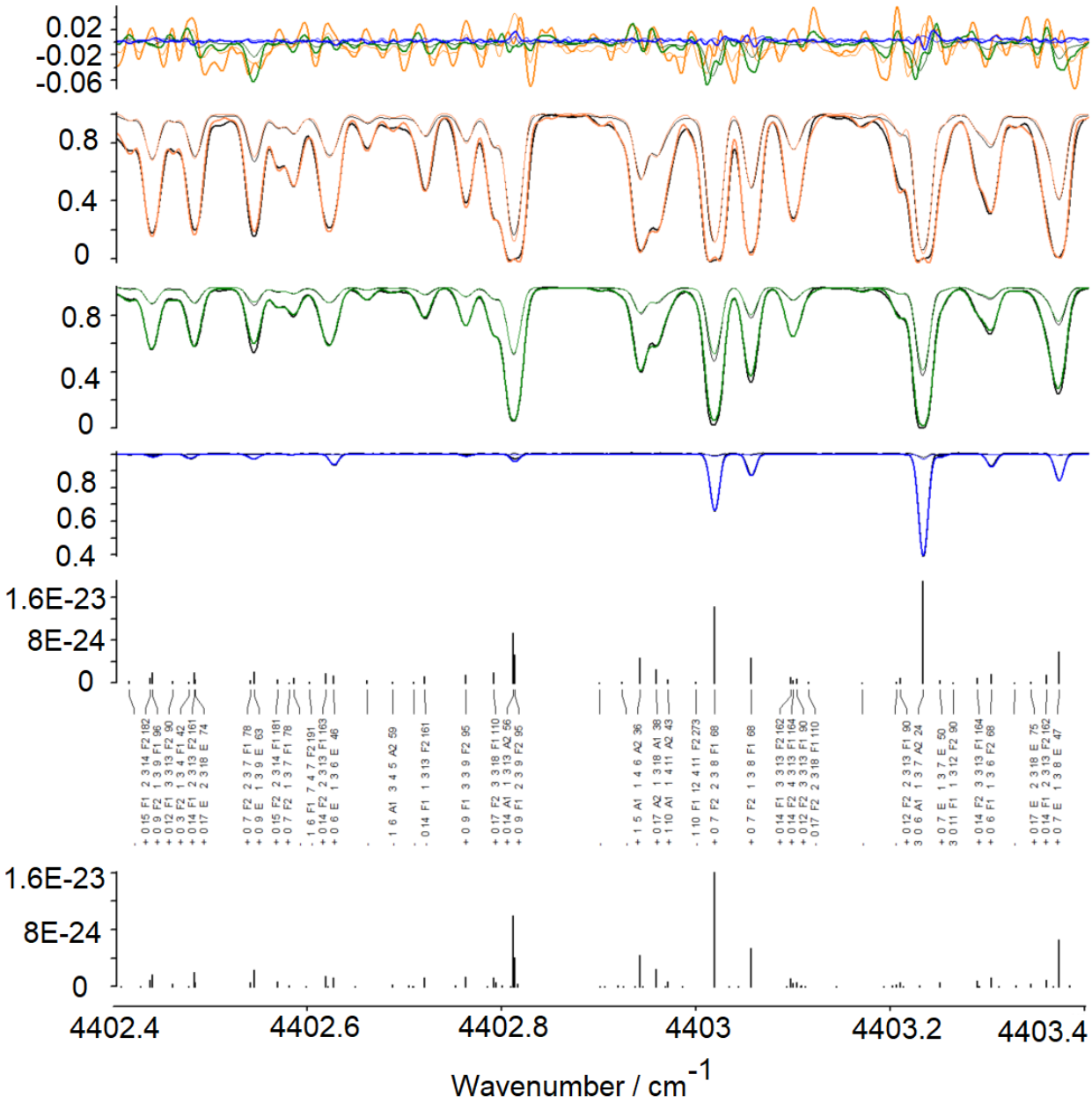

Fig. 3. The same as in Fig. 2, except for the spectral region of 4402.4-4403.4 cm^{-1}

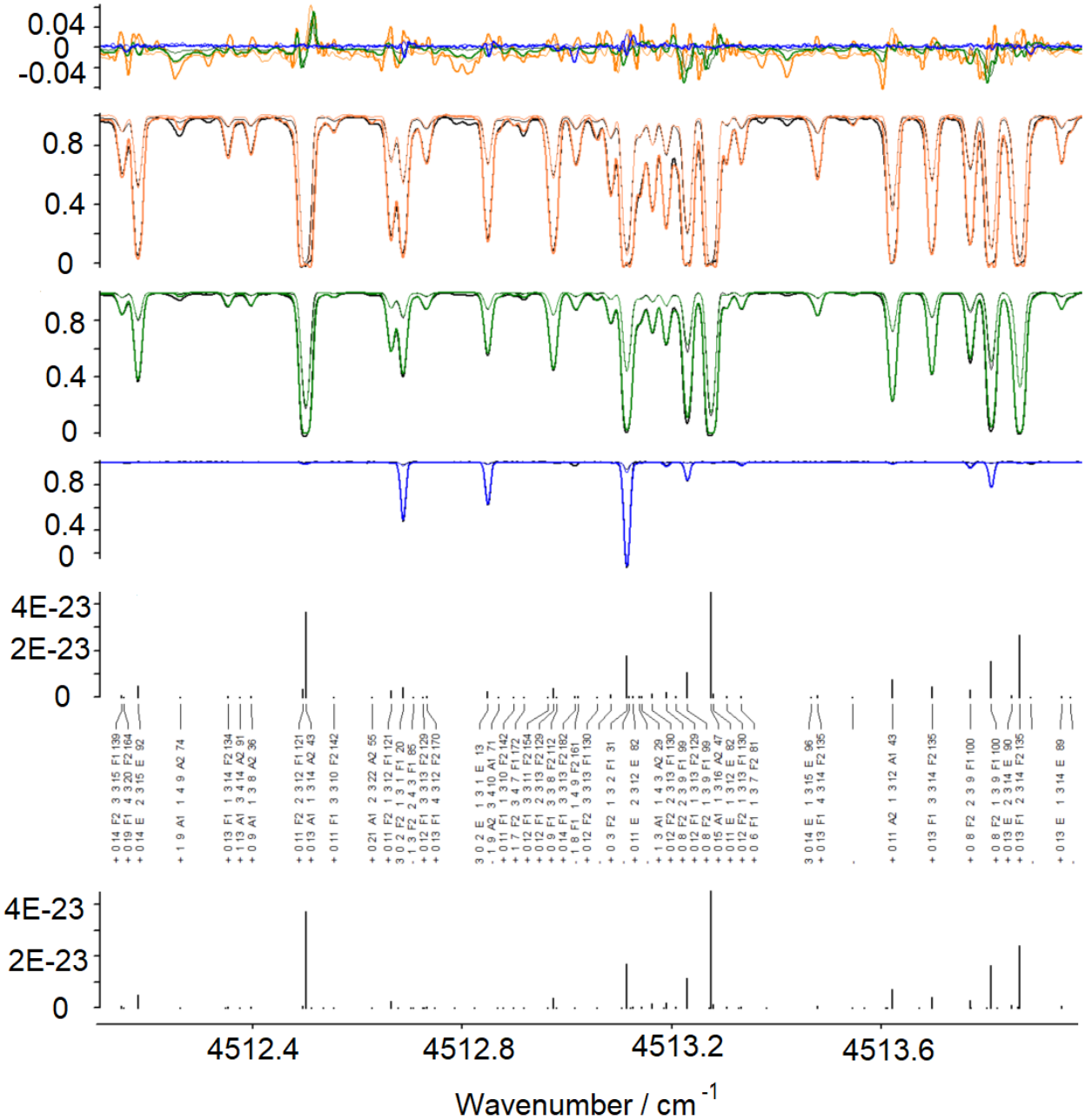

Fig. 4. The same as in Fig. 2, except for the spectral region of 4512-4514 cm^{-1}.

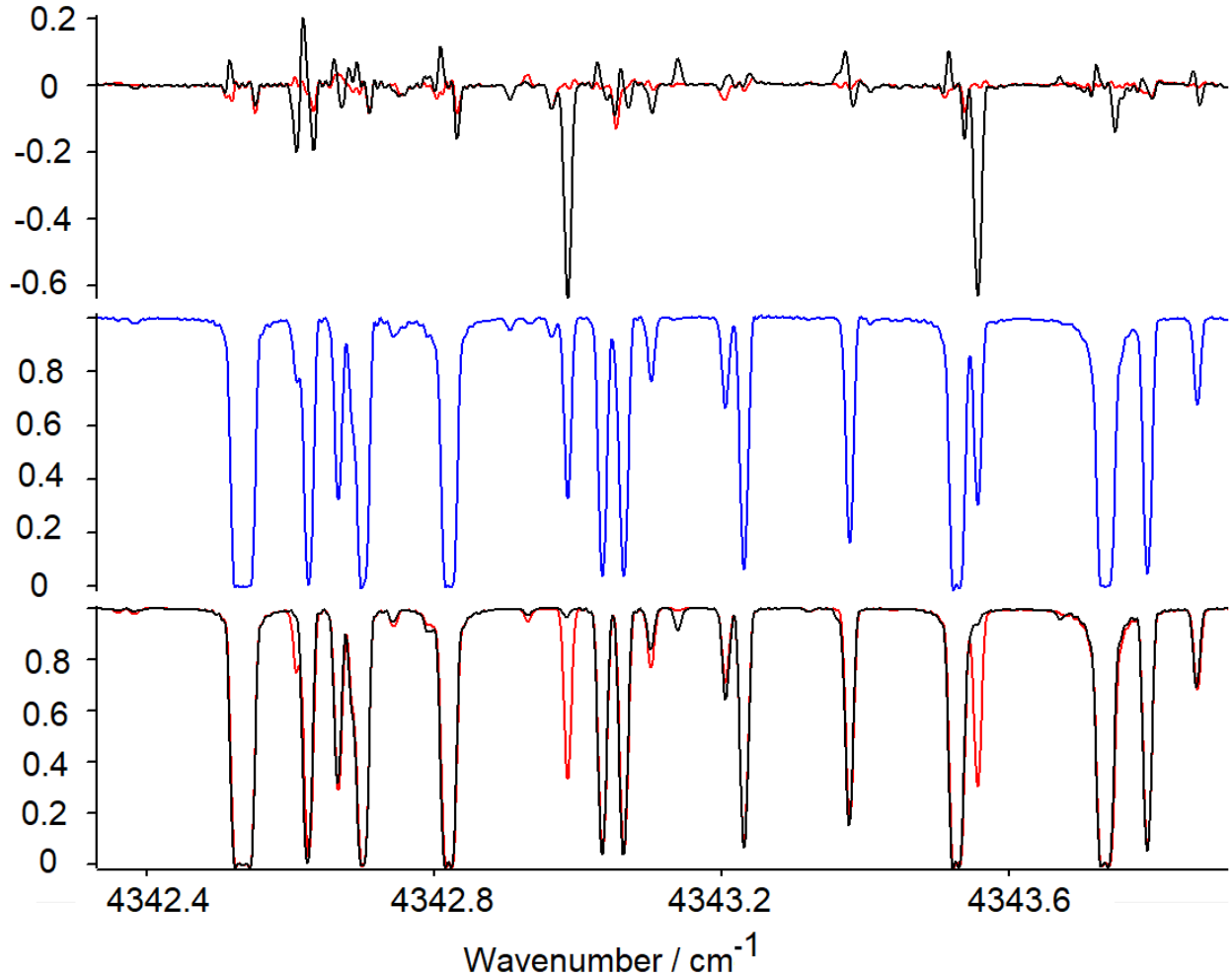

Fig. 5. *Comparison of two line lists at 123 K in the 4342 -4344 cm^{-1} range. Upper panel: residuals (obs-calc) between HITRAN2016 and observed spectra (black) and residuals for observed linelist of this work (red). Middle panel: observed spectra T (see Table2), Bottom panel: simulation using experimental linelist of this work (red) and that of HITRAN2016 (black), where some medium size lines are missing, for example, those at 4342.98 and 4343.55 cm^{-1}.*

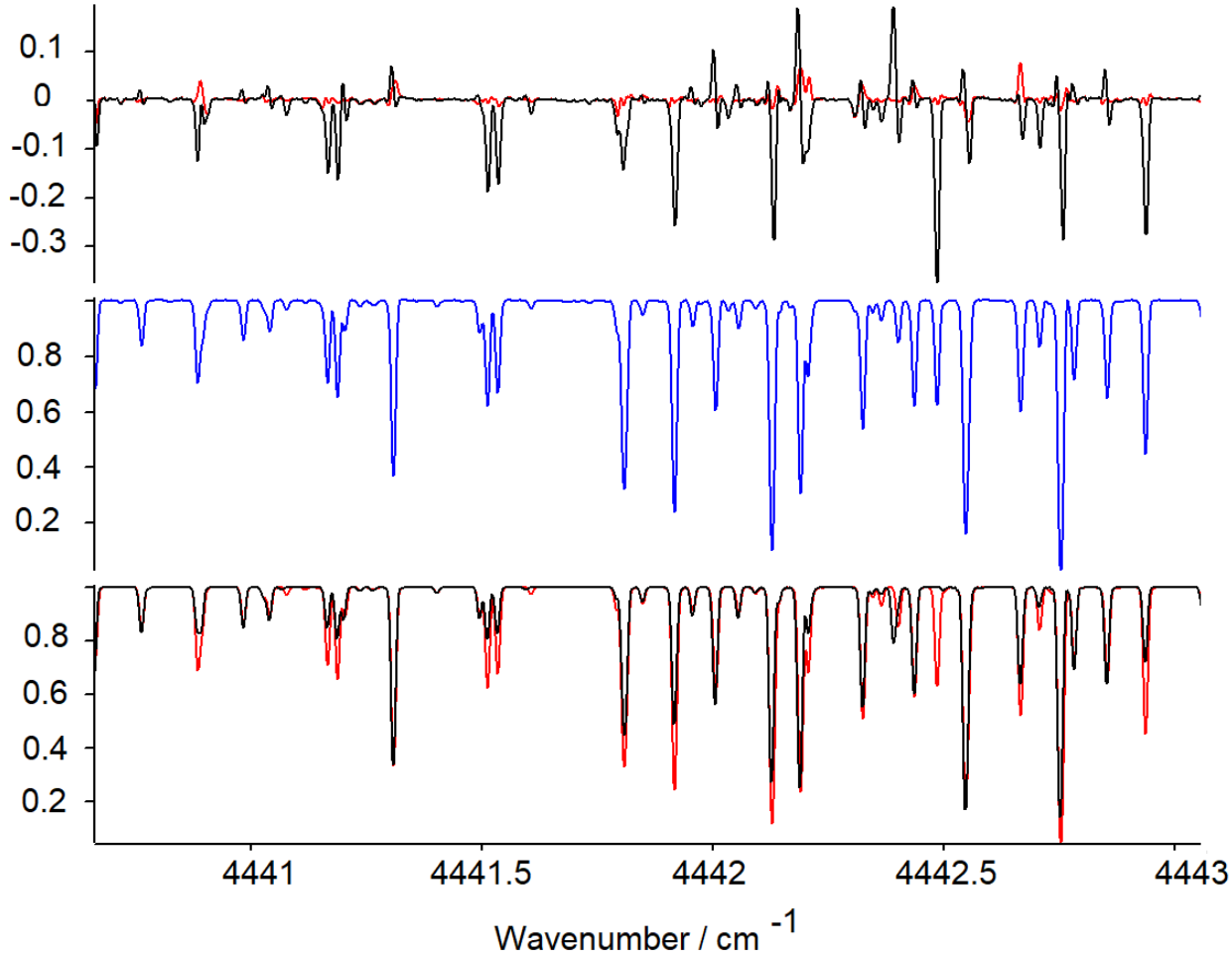

Fig. 6. *Comparison of two line lists at 123 K in the 4441-4443 cm^{-1} range. Upper panel: shows residuals (obs-calc) for HITRAN2016 and observed spectra (black) and for observed linelist of this work (red). Middle panel: observed spectra T (see Table2), Bottom below: observed linelist of this work (red) and HITRAN2016 (black), showing the HITRAN intensities are substantially off*

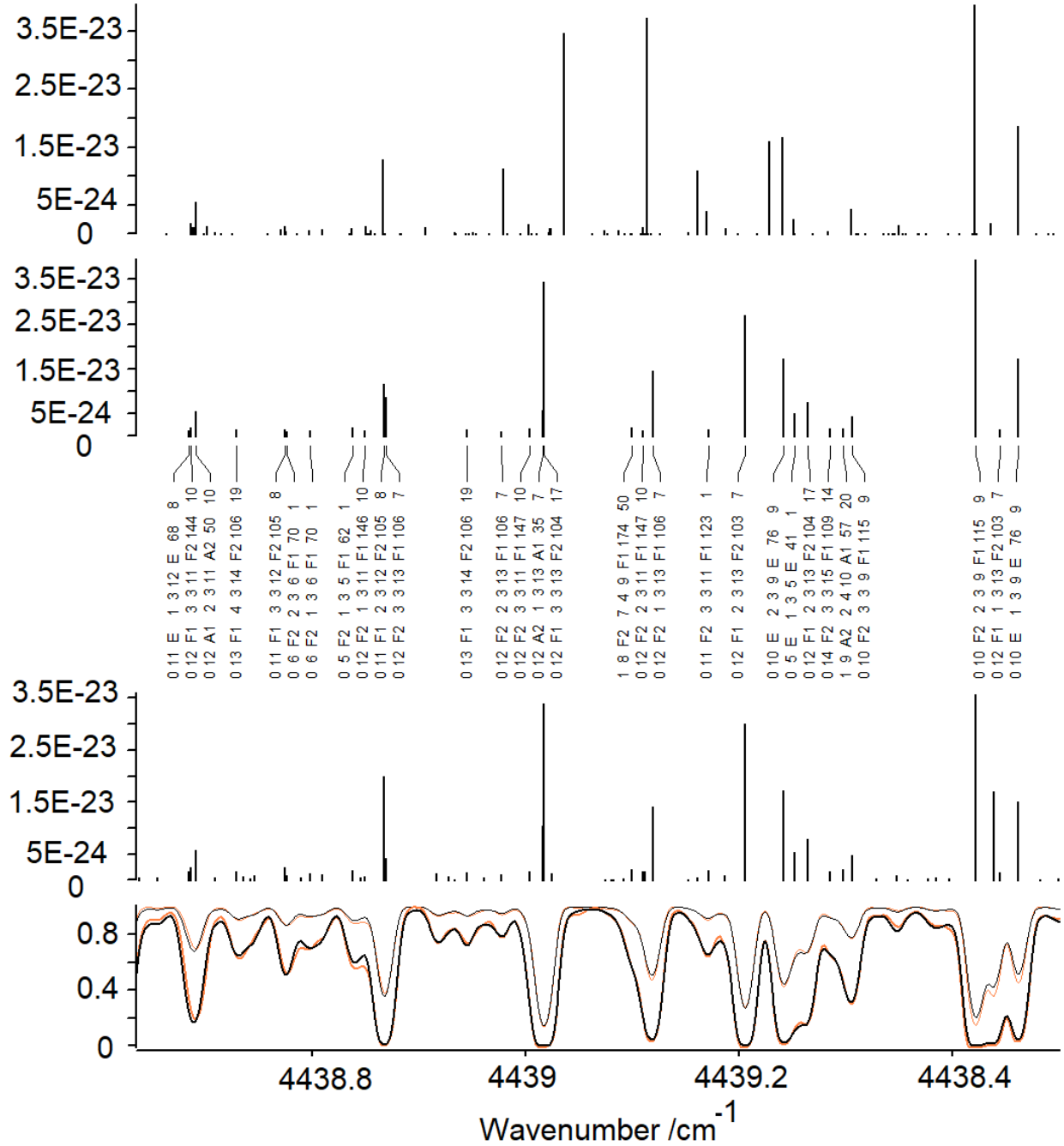

Fig. 7. *Comparison of the experimental line sticks with the calculated intensity sticks, as well as with the HITRAN 2016 data at T=290 K. The upper panel shows HITRAN2016. The lower panel shows the calculated intensity sticks. The next panel shows experimental line sticks and the lowest panel – experimental spectra for 201 m (black) and calculated spectra for 201 m .*

4. Spectra assignment

The line-by-line assignment of spectra relies on a comparison of calculated lists that contain complete quantum identifications with observed spectra. Previous works on the assignment of crowded methane spectra in the range of Octad [1] [9] have not been sufficiently complete to cover transitions of all sub-bands.

The traditional approach for spectral analyses based on effective Hamiltonian (EH) and effective dipole moment (EDM) models (see for example [37] [56] [35] and refs therein) had faced the well-known issues related to rapidly increasing number of adjustable parameters. Thanks to improved *ab initio* calculations of the potential energy surfaces (PES) and of dipole moment surfaces (DMS) [57], [50], [58], [59], [60], [61] and to global variational calculations [51] [52] , a better understanding of absorption bands in spectra of methane isotopologues has become posssible [54] [62] [63] [64] [65] . In particular, global theoretical line lists [17], [54] for astrophysical applications [66] [67] [68] [69] [70] had been generated at various temperature conditions from 50 K up to 3000 K. These theoretical studies cited above have permitted a qualitative agreement of band intensities with experiments and an improvement of predictions for the band centers [57] [60], however the accuracy of purely *ab initio* line positions is not yet sufficient for high-resolution atmospheric applications.

A recent progress in methane spectra analyses [40] [71] [72] was due to a “combined approach” [41] that comprised three steps. First, the ab initio based effective EH polyad models were derived from the molecular PES via a high order Contact Transformation (CT) method [41]. This provided realistic estimations for the coupling parameters between various rovibrational bands and for related resonance perturbations in the observed spectra. Finally, a fine tuning of a reduced set of empirically adjusted parameters permitted to extend the number of assigned lines. The formalism of irreducible tensor operators (ITO) [42] [37], implemented in the MIRS computational code [56], was used for a full account of tetrahedral symmetry properties of the methane molecule.

A more detailed discussion can be found in refs [40] [71] [43] devoted to assignments of different parts of the Tetradecad [43] [71] [72] in previous analyses. In this work, we used the most recent EH of [40] obtained via the “combined approach” [41] as an initial model to extend assignments in the present spectral range.

Table 4. Line position and intensity statistics for $^{12}CH_4$ transitions at 296 K corresponding to the studied range

Vibration upper state levels, symmetry	Vibration Energy cm^{-1} This work	Calculated from PES		Line positions				Line intensities	
		Exact KEO*, Ref [73], PES [57]	CT $^{\#}$ Ref [41], PES [74]	Number Fitted lines	*RMS* (10^{-3} cm^{-1})	J_{Min}	J_{Max}	Number Fitted Transit.	*RMS %*
(0003) F2	3870.485238	3870.506	3870.839	2	1.68	17	17	0	
(0102) E	4101.391836	4101.426	4102.026	4	2.47	15	18	2	4.19
(0102) F1	4128.763930	4128.744	4129.233	63	2.28	8	21	46	1.04
(0102) A1	4132.863475	4132.874	4133.553	27	1.60	8	19	17	9.46
(0102) F2	4142.861828	4142.810	4143.119	48	1.55	8	19	33	8.98
(0102) E	4151.202962	4151.164	4151.558	38	2.36	8	18	20	9.43
(0102) A2	4161.840387	4161.793	4162.141	61	1.71	8	18	40	8.48
(1001) F2	4223.460976	4223.566	4223.569	283	1.73	6	21	207	9.43
(0011) F2	4319.208149	4318.958	4319.412	772	1.61	0	21	607	9.91
(0011) E	4322.188360	4321.946	4322.485	598	1.43	1	21	466	1.08
(0011) F1	4322.590936	4322.351	4322.744	1090	1.45	1	21	829	1.02
(0011) A1	4322.691766	4322.429	4323.024	449	1.52	1	21	357	9.73
(0201) F2	4348.718167	4348.742	4349.458	744	1.61	0	20	423	9.75
(0201) F1	4363.607752	4363.608	4364.108	653	1.40	1	21	391	9.97
(0201) F2	4378.948765	4378.943	4379.351	693	1.49	1	21	376	1.06
(1100) E	4435.125649	4435.277	4435.232	750	1.41	1	20	436	9.29
(0110) F1	4537.550360	4537.353	4537.746	998	9.89	1	21	479	9.59
(0110) F2	4543.760944	4543.574	4544.081	1117	9.49	0	21	569	1.02
(0300) E	4592.036524	4592.117	4592.830	124	1.46	1	19	59	8.17
(0300) A2	4595.278804	4595.276	4595.667	47	1.04	1	16	17	8.00
(0300) A1	4595.515674	4595.544	4595.976	44	1.17	2	15	28	4.85
			Total	**8605**	**1.386**			**5402**	**9.9**

Notes:

*) using exact kinetic energy operator (KEO) in internal curvilinear coordinates [73]

#) using contact transformation (CT) method in normal coordinated [41]

In total, 886 EH parameters were adjusted to fit more than 34000 measured $^{12}CH_4$ line positions from the Dyad up to the lower edge of the Icosad range. It was necessary to include all this data because the parameters of low lying polyads contribute to higher polyads according to the EH polyad extrapolation scheme [37] [42] . Ten ground state 6th-order parameters were fixed to the values of Ref. [75], and 62 parameters of the Dyad were empirically optimized. Of the total number of symmetry-allowed 382, 1202, and 2539 EH 6th-order parameters specific to the Pentad, Octad, and Tetradecad, only a restricted set of 211, 279, and 329 parameters were adjusted. These samples of adjusted EH parameters correspond to the choise of our previous works [40] [72] [44]. The major sets of remaining parameters were held fixed to the theoretical predictions from the molecular PES via the CT method [41] . The obtained RMS (calculated – observed) deviation for line positions 0.0014 cm^{-1} is closed to the average descrepancies of combination differences for the upper level energy ~ 0.001cm^{-1}, obtained using several transitions .

5. The methane line list with assignments

In the Supplementary Materials of this work, we provide the line list compiled at 296 K, including quantum assignments. Table 5 shows a sample of this list . It includes the observed positions and intensities (at 296 K), the quantum assignments following the notations described in Ref [40], and lower state energies. Self-broadening and air-broadening coefficients obtained from Refs. [76] [77] were added to our final line list. More recent values of self-broadening and air-broadening coefficients in the Octad region have also been obtained in Ref. [49] (see Refs. [78] [79] [80] for the tetradecad region). Isotopic lines were identified using the line list of $^{13}CH_4$ obtained from the spectrum of enriched $^{13}CH_4$ [81] .

Table 5. *Sample of Electronic Supplementary data. Methane at 296 K with assignments in the 3760-4100 cm^{-1} region.*

Key [a]	**positions ν_0 (cm^{-1})** [b]	**Intensity cm^{-1} /(molec·cm^{-2})**	**Rotational assignment** [d]		***E_{low} estimates*** **(cm^{-1})** [e]	**Self HW** [f] **(cm^{-1}/atm)**	**Air HW** [g] **(cm^{-1}/atm)**
			Lower state	**Upper state**			
+	4300.310020	1.726e-24	0 11 F2 3	3 11 F1 84	690.017	0.069	0.0534
+	4300.320078	2.460e-25	0 16 F2 3	3 16 F1 126	1417.753	0.054	0.0316
+	4300.347522	6.940e-25	0 16 F2 4	3 16 F1 127	1418.137	0.054	0.0316
H	4300.365965	1.732e-21	0 3 A2 1	3 2 A1 8	62.878	0.079	0.0656

+	4300.386978	1.892e-23	0 14 A1 1	3 14 A2 35	1095.828	0.061	0.0416
+	4300.390664	7.933e-25	0 16 F1 3	3 17 F2 76	1417.807	0.054	0.0316
-	4300.395409	2.357e-24			814.646	0.066	0.0499
+	4300.408638	5.657e-24	0 10 E 2	3 10 E 51	575.271	0.071	0.0565
+	4300.450200	3.049e-23	0 11 F2 2	3 11 F1 84	689.876	0.069	0.0534
+	4300.456513	2.247e-23	0 11 E 1	3 11 E 55	689.886	0.069	0.0534
H	4300.459438	1.063e-22	0 12 F1 2	3 12 F2 94	814.884	0.066	0.0499
+	4300.461964	3.824e-25	1 7 F2 4	4 7 F1 120	1631.804	0.076	0.0630
+	4300.501773	2.576e-24	1 3 A1 1	4 3 A2 17	1369.017	0.079	0.0657
+	4300.502860	1.440e-24	0 16 F1 2	3 16 F2 129	1417.129	0.054	0.0316
+	4300.310020	1.726e-24	0 11 F2 3	3 11 F1 84	690.017	0.069	0.0534

Notes:

[a] *+ assigned line, - unassigned line, 3 corresponds to* $^{13}CH_4$*, H – line from HITRAN*

[b] *measured line positions.*

[c] *I(296* K): *measured line intensities* in *cm/molecule.*

[d] *Lower and upper state rovibrational assignments are given by the vibrational polyad number P, the rotational quantum number J, the rovibrational symmetry type C (T_d irreducible representation) and the rovibration ranking index α.*

[e] *E_{low}: recommended value for the lower state energy [in cm^{-1}]. Order of priority: exact assignment, lower J, observed E lower, default E lower corresponded to J=**12 (see Text).***

[f] *Self-Broadening coefficient obtained from* [76].

[g] *Air-Broadening coefficient obtained from* [77]

An overall comparison of $^{12}CH_4$ line-stick diagrams in the considered spectral range 4300-4600 cm^{-1} from the three line list is shown in Fig. 8. This includes HITRAN2016 [29], experimental list of the present work, and the ab initio born list of TheoReTS database [**58**] produced by variational calculations. At this large scale of Fig. 8, all line lists look similar. However, the detailed comparisons of observed and calculated spectra shown in Fig. 5 - 7 reveals considerable differences for medium and weak lines between the HITRAN2016 list and this work.

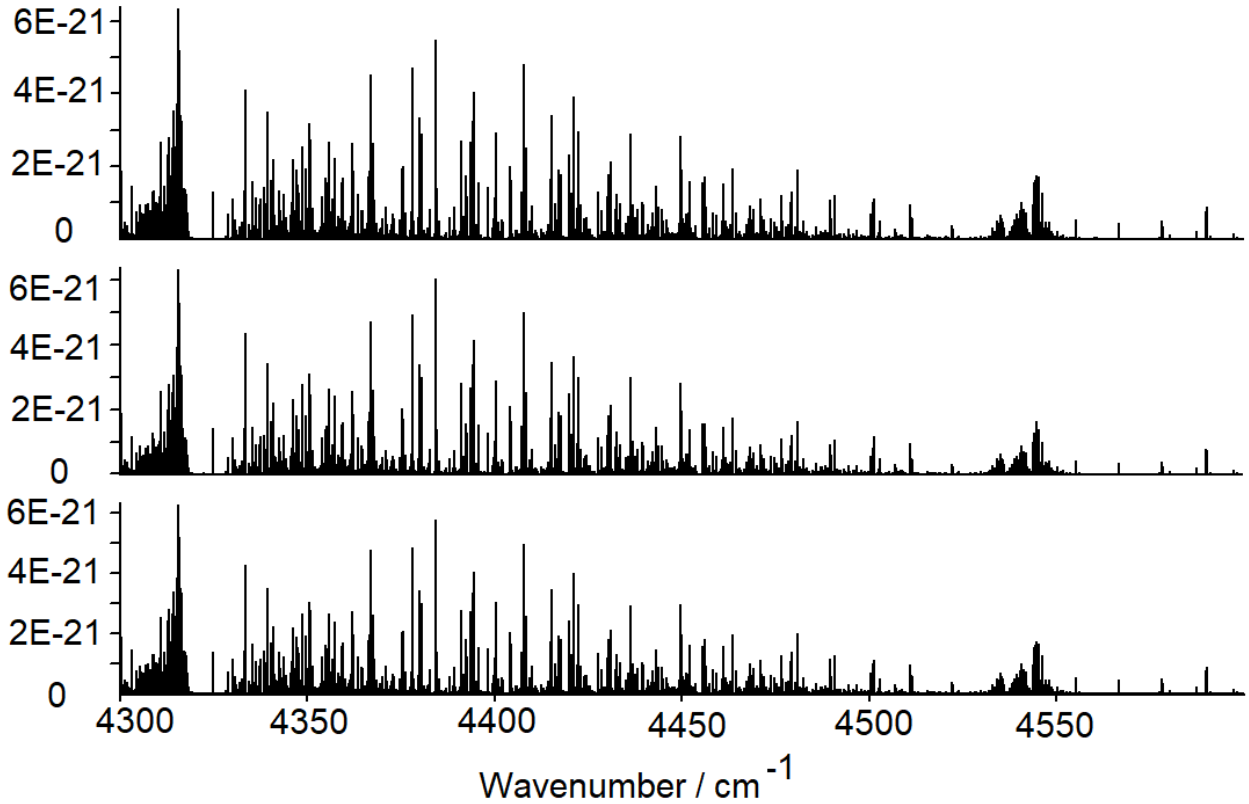

Fig. 8 *Line stick diagrams obtained from four line lists in the 4300-4600 cm^{-1} range. From top downward: HITRAN2016; This work (observed line list); Variational calculations from TheoReTS* [54] *based on ab initio dipole moment* [55].

6. Conclusion

The main results of the present spectrum analysis in the 4300-4600 cm^{-1} region are the extended assignments and improved line lists provided in the Supplementary Materials. More than 7000 new lines of $^{12}CH_4$ up to J = 21 were assigned in experimental FTS spectra recorded at various temperatures using a combined approach involving ab initio calculations with subsequent empirical optimization of the effective model. Upper state energy levels were obtained using empirical adjustment of a restricted subset of EH parameters, which were statistically well-determined in the fit. This approach allowed us to find our several significant outliers in available compilations of methane line lists in this range based on previous empirical extrapolations. These results will permit including new assignments in a forthcoming updates of HITRAN [29] and GEISA [30] spectroscopic databases.

Acknowledgments

The supports of the CNRS (France) in the frame of "Laboratoire International Associé SAMIA", of the French ANR project e-PYTHEAS (ref: ANR-16-CE31-0005), of the ROMEO computer center Reims-Champagne-Ardenne and of Academic D.Mendeleev program of Tomsk State

University (Russia) are acknowledged. Part of the research was performed at Institute of Monitoring of Climatic and Ecological Systems under contract of Russian Science Foundation (RSF), grant No. 19-77-10046. Part of the research was performed at the Jet Propulsion Laboratory, California Institute of Technology, under contract with the National Aeronautics and Space Administration. Part of the research was performed at Synchrotron SOLEIL (Project 99180032).

References

[1] Hilico J.-C., Robert O., Loлte M., Toumi S., Pine A.S., Brown L.R., Analysis of the interacting octad system of 12CH4 *J. Molec. Spectrosc.* 2001;208: 1-13.

[2] Albert S., Bauerecker S., Boudon V., Brown L.R., Champion J.-P., Loete M., Nikitin A.V., Quack M., Global analysis of the high resolution infrared spectrum of methane 12CH4 in the region from 0 to 4800 cm-1. *Chem Phys* 2009;358: 131-146.

[3] Nikitin A.V., Boudon V., Wenger Ch., Albert S., Brown L.R., Bauerecker S., Quack M., High resolution spectroscopy and the first global analysis of the Tetradecad region of methane 12CH4. *PCCP* 2013;15, no. 25: 10071-10093.

[4] Daumont L., Nikitin A.V., Thomas X., Régalia L., Von der Heyden P., Tyuterev V., Rey M., Boudon V., Wenger C., Loëte M., Brown L.R., New assignments in the 2µm transparency window of the 12CH4 Octad band system. *J. Quant. Spectrosc. Radiat. Transfer* 2013;116: 101-109.

[5] Rodina A.A., Nikitin A.V., Thomas X., Manceron L., Daumont L., Rey M., Sung K., Tashkun S.A., Tyuterev V.G., Improved line list of 12CH4 in the 3760–4100 cm−1 region *J. Quant. Spectrosc. Radiat. Transfer.* 2019;225: 351-362.

[6] Hilico J. C., Champion J.-P., Toumi S., Tyuterev V. G., Tashkun S. A., New analysis of the pentad system of methane and prediction of the (pentad-pentad) spectrum *Journal of Molecular Spectroscopy* 1994;168: 455-476.

[7] Ouardi O., Hilico J. C., Loete M., Brown L. R., 'The hot bands of methane between 5 and 10 µm *Journal of Molecular Sprctroscopy* 1996;180: 311-322.

[8] Hashemi R., Predoi-Cross A., Nikitin A.V., Tyuterev Vl.G., Sung K., Smith M.A.H., Malathy Devi V., Spectroscopic line parameters of 12CH4 for atmospheric composition retrievals in the 4300-4500 cm-1 region *J. Quant. Spectrosc. Radiat. Transfer* 2017;186: 106-117.

[9] Brown L.R., Sung K., Benner D.C., Devi V.M., Boudon V., Gabard T., et al., Methane line parameters in the HITRAN2012 database. *J. Quant. Spectrosc. Radiat. Transfer* 2013;130: 201-219.

[10] Bernath P.F., Molecular opacities for exoplanets *Phil. Trans. R Soc. A* 2014;372: 20130087.

[11] Tinetti G., Encrenaz T., Coustenis A., Spectroscopy of planetary atmospheres in our Galaxy *Astron Astrophys Rev* 2013;21, no. 1: 63.

[12] Fulchignoni M., Ferri F., Angrilli F., Ball A.J., Barn-Nun A., Barucci M.A., In situ measurements of the

physical characteristics of Titan's environment. *Nature* 2005;438: 785-790.

[13] Coustenis A., Jennings D.E., Nixon C.A., Achterberg R.K., Lavvas P., Vinatier S., Teanby N.A., Bjoraker G.L., Carlson R.C., Piani L., Bampasidis G., Flasar F.M., Romani P.N., Titan trace gaseous composition from CIRS at the end of the Cassini-Huygens prime mission. *Icarus* 2010;207: 461-476.

[14] De Bergh C., Courtin R., Bézard B., Coustenis A., Lellouch E., Hirtzig M., Rannou P., Drossart P., Campargue A., Kassi S., Wang L., Boudon V., Nikitin A., Tyuterev V., Applications of a new set of methane line parameters to the modeling of Titan's spectrum in the 1.58 µm window *Plan. Space Sci.* 2012;61, no. 1: 85-98.

[15] Hirtzig M., Bézard B., Lellouch E., Coustenis A., de Bergh C., Drossart P., Campargue A., Boudon V., Tyuterev V., Rannou P., Cours T., Kassi S., Nikitin A., Mondelain D., Rodriguez S., Le Mouélic S., Titan's surface and atmosphere from Cassini/VIMS data with updated methane opacity. *Icarus* 2013;226, no. 1: 470-486.

[16] Bezard B., The methane mole fraction in Titan's stratosphere from DISR measurements during the Huygens probe's descent. *Icarus* 2014;242: 64-73.

[17] Rey M, Nikitin A.V., Bézard B., Rannou P., Coustenis A., Tyuterev V.G., New accurate theoretical line lists of 12 CH 4 and 13 CH 4 in the 0–13400 cm−1 range: Application to the modeling of methane absorption in Titan’s atmosphere *Icarus* 2018;303: 114-130.

[18] Buchwitz M., De B.R., Noel S., Burrows J.P., Bovensmann H., Schneising O., Khlystova I., Bruns M., Bremer H., Berga-maschi P., Korner S., Heimann M., Atmospheric carbon gases retrieved from SCIAMACHY by WFM-DOAS: version 0.5 CO and CH4 and impact of calibration improvements on CO2 retrieval. *Atmos Chem Phys* 2006;6: 2907-2918.

[19] Frankenberg C., Meirink J.F., Bergamaschi P., Goede A.P. H., Heimann M., Korner S., Platt U., Van W.M., Wagner T., Satellite chartography of atmospheric methane from SCIAMACHY on board ENVISAT: Analysis of the years 2003 and 2004. *J Geophys Res* 2006;111.

[20] Bergamaschi P., Frankenberg C., Meirink J.F., Krol M., Den-tener F., Wagner T., Platt U., Kaplan J., Korner S., Heimann M., et al., Satellite chartography of atmospheric methane from SCIAMACHY on board ENVISAT: 2. Evaluation based on inverse model simulations. *J Geopphys Res* 2007;112.

[21] Schneising O., Buchwitz M., Burrows J.P., Bovensmann H., Bergamaschi P., Peters W., Three years of greenhouse gas column-averaged dry air mole fractions retrieved from satellite –Part 2: Methane. *Atmos Chem Phys Discuss* 2008;8: 8273-8326.

[22] Nisbet E.G., Dlugokencky E.J., Manning M.R., Lowry D., Fisher R.E., France J.L., al. et, Rising atmospheric methane: 2007–2014 growth *Global Biogeochemical Cycles* 2016;30: 1356-1370.

[23] Sromovsky L.A., Fry P.M., Boudon V., Campargue A., Nikitin A., Comparison of line-by-line and band models of near-IR methane absorption applied to outer planet atmospheres. *Icarus* 2012;218: 1-23.

[24] Ulenikov O.N., Bekhtereva E.S., Albert S., Bauerecker S., Niederer H.M., Quack M., Survey of the high resolution infrared spectrum of methane (12CH4 and 13CH4): Partial vibrational assignment

extended towards 12 000 cm-1 *J. Chem. Phys.* 2014;141, no. 23: 234302.

[25] Campargue A, Leshchishina O, Wang L, Mondelain D, S. Kassi, The WKLMC empirical line lists (5852-7919 cm-1) for methane between 80 K and 296 K: "final" lists for atmospheric and planetary applications. *J. Molec. Spectrosc.* 2013;291: 16-22.

[26] Brown L.R., Empirical line parameters of methane from 1.1 to 2.1 µm *J. Quant. Spectrosc. Radiat. Transfer* 2005;96: 251-270.

[27] Rey M., Nikitin A.V., Tyuterev V.G., Ab initio variational predictions for understanding highly congested spectra: Rovibrational assignment of 108 new methane sub-bands in the icosad range (6280-7800 cm-1) *Phys. Chem.Chem. Phys.* 2016;16: 176-189.

[28] Niederer H.M., Wang X.-G., Carrington T., Albert S., Bauerecker S., Boudond V., Quack M., Analysis of the rovibrational spectrum of 13CH4 in the Octad range. *J. Mol. Spectrosc.* 2013;291: 33-47.

[29] Gordon I.E., Rothman L.S., Hill C., Kochanov R.V., Tan Y., Bernath P.F., al. et, The HITRAN2016 molecular spectroscopic database. *J Quant Spectrosc Radiat Transfer* 2017;203: 3-69.

[30] Jacquinet N. , et al., The 2015 edition of the GEISA spectroscopic database *J. Molec. Spectrosc.* 2016;327: 31–72.

[31] Tyuterev Vl.G., Babikov Yu.L., Tashkun S.A., Perevalov V.I., Nikitin A.V., Champion J.P., et al., TDS spectroscopic databank for spherical tops 1994;52, no. 3/4: 459-480.

[32] Wenger C. , Champion J.-P., Spherical top data system (STDS) software for the simulation of spherical top spectra. *J. Quant. Spectrosc. Radiat. Transfer* 1998;59: 471-480.

[33] Ba Y.A., Wenger C., Surleau R., Boudon V., Rotger M., Daumont L., Bonhommeau D.A., Tyuterev V.G., Dubernet M.-L., MeCaSDa and ECaSDa: Methane and ethene calculated spectroscopic databases for the virtual atomic and molecular data centre *J. Quant. Spectrosc. Radiat. Transfer.* 2013;130: 62-68.

[34] Hargreaves R.J., Bernath P.F., Beale C.A., Dulick M., Empirical line lists and absorption cross-sections for methane at high temperatures *The Astrophysical Journal* 2015;813: 1.

[35] Amyay B., Louviot M., Pirali O., Georges R., Vander Auwera J., Boudon V., *J. Chem. Phys.* 2016;144: 024312.

[36] Toon G.G., J.-F. Blavier., Sung K, Rothman L.S., Gordon I.E., HITRAN spectroscopy evaluation using solar occultation FTIR spectra *J. Quant. Spectrosc. Radiat. Transfer.* 2016;182: 324-336.

[37] Champion J.-P., Loete M., Pierre G., *Spectroscopy of the Earth's Atmosphere and Interstellar Medium in: K.N. Rao, A.Weber (Eds.)*. San Diego: Academic Press, 1992.

[38] Nikitin A.V., Lyulin O.M., Mikhailenko S.N., Perevalov V.I., Filipov N.N., Grigoriev I.M., Morino I., Yokota T., Kumazawa R., Watanabe T., GOSAT-2009 methane spectral line list in the 5550–6236 cm-1 range. *J. Quant. Spectrosc. Radiat. Transfer* 2010;111: 2211-2224.

[39] Nikitin A.V., Lyulin O.M., Mikhailenko S.N., Perevalov V.I., Filippov N.N., Grigoriev I.M., Morino I., Yoshida Y., Matsunaga T., GOSAT-2014 methane spectral line list *J. Quant. Spectrosc. Radiat. Transfer.* 2015;154: 63–71.

[40] Nikitin A.V., Thomas X., Daumont L., Rey M., Sung K., Toon G.C., Smith M.A.H., Mantz A.W., Tashkun S.A., Tyuterev Vl.G., Measurements and modeling of long-path 12 CH 4 spectra in the 5300–5550 cm −1 region *J. Quant. Spectrosc. Radiat. Transfer* 2017;202: 255–264.

[41] Tyuterev Vl.G., Tashkun S.A., Rey M., Kochanov R.V., Nikitin A.V., Delahaye T., Accurate spectroscopic models for methane polyads derived from a potential energy surface using high-order contact transformations. *The Journal of Physical Chemistry* 2013;117: 13779−13805.

[42] Zhilinskii B.I., Perevalov V.I., Tyuterev Vl.G., *Method of Irreducible Tensorial Operators in the Theory of Molecular Spectra*. Novosibirsk: Nauka, 1987.

[43] Nikitin A.V., Thomas X., Regalia L., Daumont L., Rey M., Tashkun S.A., Tyuterev Vl.G., Brownc L.R., Measurements and modeling of long-path 12CH4 spectra in the 4800-5300 cm-1 region *J. Quant. Spectrosc. Radiat. Transfer* 2014;138: 116–123.

[44] Nikitin A.V., Thomas X., Daumont L., Rey M., Sung K., Toon G.C., Smith M.A.H., Mantz ProtasevichA.E., A.W., Tashkun S.A., Tyuterev Vl.G., Assignment and modelling of 12CH4 spectra in the 5550–5695, 5718–5725 and 5792–5814 cm−1 regions *J. Quant. Spectrosc. Radiat. Transfer* 2018;219: 323–332.

[45] Nikitin A.V., Thomas X., Regalia L., Daumont L., Von der Heyden P., Tyuterev Vl.G., First assignment of the 5v4 and v2+4v4 band systems of 12CH4 in the 6287-6550 cm-1 region. *J. Quant. Spectrosc. Radiat. Transfer* 2011;112: 28-40.

[46] Tchana F.K., Willaert F., Landsheere X., Flaud J.-M.,Lago,L., Chapuis M., Herbeaux C., Roy P, Manceron L, A new, low temperature long-pass cell for mid-infrared to terahertz spectroscopy and synchrotron radiation use *REVIEW OF SCIENTIFIC INSTRUMENTS* 2013;84: 093101.

[47] Lago L., Herbeaux C., Bol M., Roy P., Manceron L., A rugged, high precision capacitance diaphragm low pressure gauge for cryogenic use *Rev. Sci. Inst.* 2014;85: 015108.

[48] Nikitin A.V. , Kochanov R.V.Visualization and identification of spectra by the SpectraPlot, Visualization and identification of spectra by the SpectraPlot program. *Atmos Ocean Opt* 2011;24: 931-941.

[49] Devi V.M., Benner D.C., Smith M.A., Mantz A.W., Sung K., Crawford T.J., Predoi-Cross A., Self- and air-broadened line shape parameters in the v2+v3 band of 12CH4: 4500–4630 cm-1 *J. Quant. Spectrosc. Radiat. Transfer.* 2015;52: 149–165.

[50] Nikitin A.V., Rey M., Tyuterev V.G., New dipole moment surfaces of methane. *Chem. Phys.Lett.* 2013;565, no. 5: 5-11.

[51] Rey M., Nikitin A.V., Tyuterev Vl.G., First principles intensity calculations of the methane

rovibrational spectra in the infrared up to 9300 cm-1. *PCCP* 2013;15, no. 25: 10049-10061.

[52] Rey M., Nikitin A.V., Tyuterev Vl.G., Convergence of normal mode variational calculations of methane spectra: Theoretical line list in the icosad range computed from potential energy and dipole moment surfaces *J. Quant. Spectrosc. Radiat. Transfer.* 2015;164: 207–220.

[53] Rey M., Nikitin A.V., Tyuterev V.G., Complete nuclear motion Hamiltonian in the irreducible normal mode tensor operator formalism for the methane molecule *J. Chem. Phys* 2012;136, no. 24: 244106.

[54] Rey M., Nikitin A.V., Babikov Y., Tyuterev Vl.G., TheoReTS – An information system for theoretical spectra based on variational predictions from molecular potential energy and dipole moment surfaces *J. Molec. Spectrosc.* 2016;327: 138–158.

[55] Nikitin A.V., Rey M., Tyuterev Vl.G., Accurate line intensities of methane from first-principles calculations *J. Quant. Spectrosc. Radiat. Transfer* 2017;200: 90-99.

[56] Nikitin A.V., Rey M., Champion J.-P., Tyuterev Vl.G., Extension of the MIRS computer package for modeling of molecular spectra: from effective to full ab initio ro-vibrational hamiltonians in irreducible tensor form. *J. Quant. Spectrosc. Radiat. Transfer* 2012;113: 1034-1042.

[57] Nikitin A.V., Rey M., Tyuterev Vl.G., First fully ab initio potential energy surface of methane with a spectroscopic accuracy *J. Chem. Phys.* 2016;145: 114309.

[58] Cassam-Chenai P. , Lievin J, Ab initio calculation of the rotational spectrum of methane vibrational ground state *J. Chem. Phys.* 2012;136: 174309.

[59] Cassam-Chenaï P. , Liévin J., An improved third order dipole moment surface for methane *J. Molec. Spectrosc.* 2013;291: 77–84.

[60] Owens A., Yurchenko S.N., Yachmenev A., Tennyson J., Thiel W., A highly accurate ab initio potential energy surface for methane *J. Chem. Phys.* 2016;145: 104305.

[61] Majumder M, Hegger S.E., Dawes R., Manzhos S., Wang X.-G., Carrington T.Jr., J. Lid, Guo H., Explicitly correlated MRCI-F12 potential energy surfaces for methane fit with several permutation invariant schemes and full-dimensional vibrational calculations *Molecular Physics* 2015;113, no. 13: 1823-1833.

[62] Rey M., Nikitin A.V., Tyuterev V.G, Predictions for methane spectra from potential energy and dipole moment surfaces: Isotopic shifts and comparative study of 13CH4 and 12CH4. *J. Mol. Spectrosc.* 2013;291: 85-97.

[63] Rey M., Nikitin A.V., Tyuterev Vl.G., First Predictions of Rotationally Resolved Infrared Spectra of Di-Deuteromethane (12CH2D2) From Potential Energy and Dipole Moment Surfaces *J Phys Chem A* 2015;119: 4763−4779.

[64] Rey M., Nikitin A.V., Tyuterev Vl.G., Accurate first-principles calculations for 12CH3D infrared spectra from isotopic and symmetry transformations *J. Chem. Phys.* 2014;141: 044316.

[65] Starikova E., Nikitin A.V., Rey M., Tashkun S.A., Mondelain D., Kassi S., Campargue A., Tyuterev V., Assignment and modeling of the absorption spectrum of 13CH4 at 80K in the region of the 2v3 band (5853-6201cm-1) *J. Quant. Spectrosc. Radiat. Transfer.* 2016;177: 170-180.

[66] Rey M., Nikitin A.V., Tyuterev Vl.G., THEORETICAL HOT METHANE LINE LISTS UP TO T = 2000 K FOR ASTROPHYSICAL APPLICATIONS *The Astrophysical Journal* 2014;789: 1.

[67] Rey M., Nikitin A.V., Tyuterev V.G., Accurate Theoretical Methane Line Lists in the Infrared up to 3000 K and Quasi-continuum Absorption/Emission Modeling for Astrophysical Applications *Astrophysical journal* 2017;847: 105.

[68] Yurchenko S.N. , Tennyson J., ExoMol line lists-IV. The rotation-vibration spectrum of methane up to 1500 K *Monthly Notices of the Royal Astronomical Society* 2014;440: 1649-1661.

[69] Yurchenko S.N., Amundsen D.S., Tennyson J., Waldmann I.P., A hybrid line list for CH 4 and hot methane continuum *Astronomy and Astrophysics* 2017;605: A95.

[70] Hargreaves R.J., Gordon I.E., Rey M, Nikitin A.V., Tyuterev V.G., Kochanov R.V., Rothman L.S., An Accurate, Extensive, and Practical Line List of Methane for the HITEMP Database *The Astrophysical Journal Supplement Series* 2020;247: 55.

[71] Nikitin A.V., Chizhmakova I.S., Rey M., Tashkun S.A., Kassi S., Mondelain D., Campargue A., Tyuterev Vl.G., Analysis of the absorption spectrum of 12CH4 in the region 5855-6250 cm-1 of the 2v3 band *J. Quant. Spectrosc. Radiat. Transfer.* 2017: https://doi.org/10.1016/j.jqsrt.2017.05.014.

[72] Ghysels M., Mondelain D., Kassi S., Nikitin A.V., Rey M., Campargue A., The methane absorption spectrum near 1.73 µm (5695–5850 cm −1): Empirical line lists at 80 K and 296 K and rovibrational assignments *JQSRT* 2018;213: 169–177.

[73] Nikitin A.V., Rey M., Tyuterev Vl.G., An efficient method for energy levels calculation using full symmetry and exact kinetic energy operator: tetrahedral molecules *J. Chem. Phys.* 2015;142: 094118.

[74] Nikitin A.V., Rey M., Tyuterev Vl.G., Rotational and vibrational energy levels of methane calculated from a new potential energy surface *Chem. Phys. Lett.* 2011;501: 179-186.

[75] Champion J.P., Hilico J.C., Brown L.R., The vibrational ground state of 12CH4 and 13CH4 *Journal of Molecular Spectroscopy* 1989;133, no. 2: 244-255.

[76] Lyulin O.M., Perevalov V.I., Morino I., Yokota T., Kumazawa R., Watanabe T., Measurements of self-broadening and self-pressure-induced shift parameters of the methane spectral lines in the 5556-6166 cm-1 range *J. Quant. Spectrosc. Radiat. Transfer* 2011;112: 531-539.

[77] Lyulin O.M., Nikitin A.V., Perevalov V.I., Morino I., Yokota T., Kumazawa R., Watanabe T., Measurements of N2- and O2-broadening and shifting parameters of methane spectral lines in the 5550-6236 cm-1 region *J Quant Spectrosc Radiat Transfer* 2009;110: 654-668.

[78] Devi V.M., Benner D.C., Sung K, Crawford T.J., Yu S., Brown L.R., Smith M.A.H., Mantz A.W., Boudon

V., Ismail S., Self- and air-broadened line shapes in the 2v3 P and R branches of 12CH4 *J. Molec. Spectrosc.* 2015;315: 114–136.

[79] Devi V.M., Benner D.C., Sung K, Brown L.R., Crawford T.J., Yu S., Smith M.A.H., Mantz A.W., Boudon V., Ismail S., Spectral line parameters including line shapes in the 2v3 Q branch of 12CH4 *J. Quant. Spectrosc. Radiat. Transfer* 2016;77: 152–169.

[80] Kochanov V.P. , Morino I., Methane line shapes and spectral line parameters in the 5647 – 6164 cm−1 region *J. Quant. Spectrosc. Radiat. Transfer* 2018;206: 313-322.

[81] Brown L.R., Nikitin A.V., Sung K., Rey M., Tashkun S.A., Tyuterev V., Crawford T.J., Smith M.A.H., Mantz A.W., Measurements and modeling of cold 13CH4 spectra in the 3750-4700 cm-1 region *J. Quant. Spectrosc. Radiat. Transfer.* 2016;174: 88-100.